Tellus (1998), 50A, 468–489
Printed in UK – all rights reserved

TELLUS
ISSN 0280–6495

Numerical simulations of sea and land breezes at high latitudes

By SIGBJØRN GRØNÅS* and ANNE DAGRUN SANDVIK, [1]*Geophysical Institute, University of Bergen, Allégaten 70, 5007 Bergen, Norway*

(Manuscript received 13 January 1997; in final form 29 April 1998)

ABSTRACT

Few investigations of sea/land breezes (SB/LB) at high latitudes have been reported in the meteorological literature. However, internal reports at some Norwegian institutions, summarised recently by Grønås and Sandvik, show that SB/LBs, in combination with terrain-driven circulations, are frequent along the coast of Norway and Spitsbergen. In this paper, numerical simulations of SB/LBs for latitudes between 50° and 80°N have been made for spring and summer with a mesoscale non-hydrostatic model in order to study the characteristics of high latitude SB/LBs. The results show that in spring, the latitudinal variation of the extent and strength of the SB is large, and no SB seems to develop north of 70°N. The LB is active at all latitudes and increases in strength and duration with increasing latitudes. In summer it is found that the character of the SB changes from a classical SB at 50°N to a monsoon kind of a SB at the highest latitudes with small diurnal variations. The northward decrease in the extent and strength of the SB is small. The results are found to be in accord with observations. The high latitude SB in summer is further studied by simulations on a circular island at 78°N. A relatively strong SB develops which persists during the night with a stronger circulation the next day. In this way, what we have called a monsoon low SB establishes over the island. The influence of an snow/ice cover and mountains has been investigated. It is indicated from both simulations and observations that monsoon lows might be present at peninsulas and islands at latitudes down to at least 60°N.

1. Introduction

Among the most popular subjects studied by meteorologists are the phenomena of sea and land breeze (SB and LB). Terrain-driven circulations of similar nature to SB/LB work in concert with them, and in nature and observational studies it might be hard to separate the phenomena of SB/LB from terrain-driven circulations. An overview of theories of SB/LB and other similar thermal circulations, and investigations based on observations and numerical simulations, has been given by Atkinson (1981). Nearly all research reported in meteorological journals has been limited to low- and mid-latitudes. However, some observational evidence of high latitude SB/LB is found in internal reports at several research institutions in Norway. A summary of the findings has recently been given by Grønås and Sandvik (1996).

SB/LBs and terrain-driven circulations are indeed frequent along the coast of Norway, and in July SBs are observed at Spitsbergen at nearly 80°N. The climate is here sufficiently warm to melt the snow and the ice in summer which accumulate during winter. The main reason for the mild climate is the warm Norwegian Atlantic Current, which flows close to the coast of Norway and up to Spitsbergen. This current has no counterpart anywhere else in Arctic regions. The significance of the warm current is reflected in the high

* Corresponding author.

northern position of the edge of the sea ice, which is shown for winter and summer in Fig. 1 (drawn from Hanssen-Bauer et al., 1990).

The SB at high latitudes is limited to the spring and summer seasons, the only time of the year when the land becomes appreciably warmer than the sea during the day. The great length of the summer day gives the SB a long duration at the expense of the LB. The frequent occurrence of the SB (combined with terrain-driven circulations) along the coast of Norway in summer, and its long duration, causes the prevailing wind direction to be along the coast, with land to the left, in the fjords and up the valleys (Grønås and Sandvik, 1996). In winter, when the land most of the time is colder than the sea, the opposite wind directions are dominating. In this way the influence of high-latitude SB/LB results in a monsoon with prevailing onshore wind in summer and wind from land in winter. In Godske et al. (1957), it is

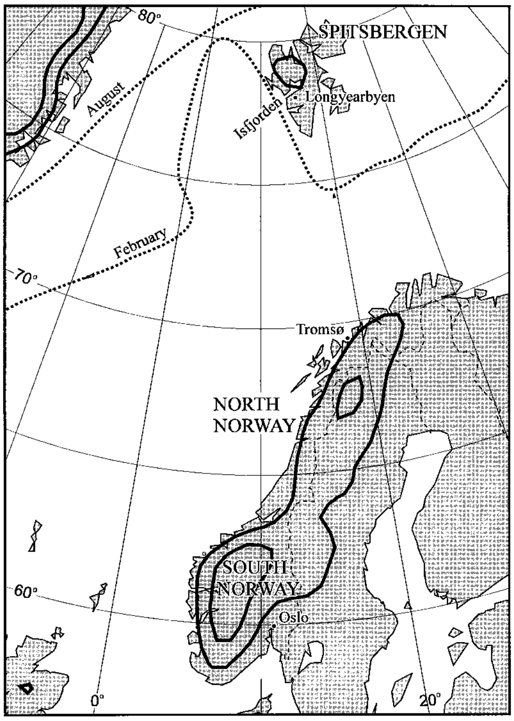

Fig. 1. Map of Norway and Spitsbergen with some geographical names and topography contours of 500 and 1000 m. Marked is the mean maximum sea-ice extent in late winter and mean minimum extent in late summer (taken from Hanssen-Bauer et al. (1990)).

indicated that the low pressure anomaly over land connected to a SB might endure during the night. In this way a low, which they called a monsoon low, might be established over high latitude islands or peninsulas, e.g., South Norway and Iceland. Such lows have been reported at Spitsbergen in July (Grønås and Sandvik, 1996) to give wind in Isfjorden (Fig. 1) both day and night for periods of several days.

At high latitudes, the mountains might be snow-covered most of the summer and glaciers are common. In Arctic regions, glaciers are extensive and reach often down to the sea surface. The existence of snow and ice might in summer cause a local circulation from these cold areas to warmer dry surroundings free of snow and ice. Such a circulation, which belongs to the non-classical mesoscale circulations (Segal and Arritt, 1992), will have characteristics of the SB and has been called snow breeze (Johnson et al., 1984). The circulation will be modified considerably by katabatic winds on sloping elevations covered with snow/ice, which normally are present in such areas. Observational evidence of such winds has been given from Greenland by Oerlemans and Vugts (1993). The down-slope winds are dominant both day and night, but a clear diurnal variation is observed. Simultaneously, on lower, snow-free slopes near the coast a combination of SB and valley wind might develop. Where the two systems meet, upward motions into the free atmosphere might be increased, and convective clouds might be formed (Bergeron, 1934). An example of such a case in spring over South-Norway has been given in Grønås and Sandvik (1997).

The physical mechanisms of the classical SB/LB are well-known. The land at clear sky in summer is heated to a much greater degree than the sea during the day. The air above the land will also be heated and ascended. Cooler air of the SB flows in to supply its place. During the night the temperature over the land surface and the air above drops below that of the sea. Thus the air becomes heavier and we get a denser flow out over the sea as LB. The structure and extent of the SB/LB have been investigated theoretically by several using linear theory. Rotunno (1983) gives a historical review of such work and extends the theory on the variation of the SB structure with latitude for days with equal length of day and night. A similar, slightly different theory has been given by Niino (1987). The Coriolis force plays an important role and gives a well known clockwise rotation (northern Hemisphere) of the wind vector with time. Both theories predict that the latitudinal variation of the vertical component of planetary vorticity (Coriolis parameter f) has a substantial effect on the structure of the systems and makes them decrease in strength and extent towards higher latitudes. Arrit (1989) found that Rotunno's theory agrees well with numerical simulations of SB/LBs for mid-latitudes. However, no data has been available to confirm the theories for high latitudes.

The special insolation conditions, and the large Coriolis parameter modify the SB/LB circulations at high latitudes compared to those at mid-latitudes. In this paper we do idealised simulations with a non-hydrostatic numerical model to gain a better understanding of the high latitude SB/LB. A main object is to study how the structures change with latitude and season from spring to summer. The special summer SB at very high latitudes, which lasts both day and night, are further studied for a circular island, which is supposed to give more realistic settings for an arctic island like Spitsbergen. We also make a few numerical experiment to study the modifying effects on the SB/LB of terrain-driven circulations and non-classical circulations between surfaces with and without a cover of snow or ice.

Numerical studies of SB and related circulations at low- and mid-latitudes have been numerous. Accounts of papers have been given by Atkinson (1981), see also Simpson (1994). The first attempt on a 2-dimensional numerical model of the SB was made by Pearce (1955). Well known are the 2-dimensional model experiments by Estoque (1961, 1962). The first 3-dimensional SB model was made by McPherson (1970), however, the model was not quite successful because of the use of an unstable numerical scheme. More known are the model and the experiments by Pielke (1974). Several papers are focusing on the effect of irregularities of the coast, such as islands, peninsulas and bays (McPherson, 1970; Neuman and Mahrer, 1971, 1974, 1975; Physick, 1976, 1980; Estoque and Gross, 1981, Mahrer and Segal, 1985). Other papers centre on the effect of the orography (Mahrer and Pielke, 1977; Ookouchi et al., 1978; Neuman and Savijärvi, 1986). Anthes (1978) studied the height of the planetary boundary layer and Arritt (1989) the offshore extent of the SB. Quite many investigations have been made for specific geographical regions, examples are Kikuchi et al. (1981), Ookouchi and Wakata (1984), Tjernström and Grisogono (1996), Grisogono and Tjernström (1996).

Our experiments have been made from initial states at rest with the non-hydrostatic numerical model developed by Mousiopoulos (1989), Flassak (1990). The numerical model is briefly described in section two, and the set-up of the experiments is found in section three. Two kinds of simulations have been made. (1) Simulations of nearly 2-dimensional SB/LB systems in spring and summer for different latitudes between 50°N and 80°N. The results shown in section four address the latitudinal variation of SB/LB in spring and summer. In particular, the long duration of the SB in summer is demonstrated. (2) Experiments on a circular island in summer at 78°, a latitude representative for Spitsbergen. These simulations have been made for a further study of the monsoon-like SB found at a very high latitudes. A circular island, which is known to strengthen the SB, has been used because the SB/LB in Norway and at Spitsbergen are often connected to islands and peninsulas. The results in section five show a clear monsoon low over the island with onshore wind both day and night. The modifying effects of ice-covered areas and mountains in the middle of the island are shown. A summary and concluding remarks are found in section six.

2. The numerical model

The non-hydrostatic mesoscale numerical model MEMO has been developed at the University of Karlsruhe and has been installed at several research institutions in Europe. Detailed descriptions of the model are found in Flassak and Moussiopoulos (1987), Moussiopoulos (1989), Flassak (1990), Moussiopoulos (1994) and Kunz and Moussiopoulos (1995). The dry version of the model is in this paper used with the following dependent variables: the three wind components, pressure, potential temperature, and turbulent kinetic energy. The vertical coordinate is a normalised height. When mountains are involved, this height is measured from the top of the terrain. With the resolution used in this paper, the non-hydrostatic pressure perturbations are small, and the same results could probably have been obtained with a hydrostatic model.

Finite differences are used to solve the equation system on a staggered Arakawa C-grid. Temporal discretisation of the prognostic equations is based on the explicit second order Adams-Bashfort scheme (Flassak, 1990). There are two deviations from this: the non-hydrostatic part of the pressure perturbation is treated implicitly, and for the vertical turbulent diffusion the second order Crank-Nicolson method is used.

MEMO has a well behaved advection scheme which ensure reasonable results even for the shorter wave lengths. This is important for our kind of integrations, where the resolution sometimes is marginal. The scheme fulfils the following five requirements (Flassak, 1990): transportivity, positivity, conservativity, numerical stability and low numerical diffusion. The well known upstream scheme is frequently used in mesoscale models because of its simplicity. It fulfils the four first requirements, but has the great disadvantage of strong numerical diffusion. To avoid this problem a second-order so called total-variation-diminishing (TVD) scheme has been developed, based upon the 1D scheme proposed by Harten (1984) and (1986). This scheme combines the upstream scheme with the second order Adams-Bashfort scheme, and has little numerical diffusion.

The handling of the boundary conditions are always vital in our kind of limited area modelling, and much effort has been put in MEMO on this aspect. At open boundaries radiation conditions, Orlanski (1976), are used as boundary conditions. The original radiation conditions merely allow disturbances to propagate out through the boundaries, but do not allow information from outside to be imposed at the boundary. Therefore, expanded radiative conditions are used at the lateral boundaries, Carpenter (1982). For the non-hydrostatic part of the mesoscale pressure perturbation, homogenous Neumann boundary conditions are used at lateral boundaries.

At the upper boundary Neumann boundary conditions are imposed for the horizontal velocity components and the potential temperature. To ensure non-reflectivity, a radiative condition (Klemp and Durran, 1983) is used for the hydrostatic part of the mesoscale pressure perturbation at that boundary. Therefore, vertically propagating internal gravity waves are allowed to leave the computational domain. For the non-hydrostatic part of the mesoscale pressure perturbation, homogenous staggered Dirichlet conditions are imposed (Flassak, 1990).

The lower boundary coincides with a height above ground corresponding to its aerodynamic roughness. For the non-hydrostatic part of the pressure perturbation, inhomogeneous Neumann conditions are imposed. A discussion about Neumann and Dirichlet problems may be found in, e.g., Copson (1975). All other conditions at the lower boundary follow from the assumption that the Monin–Obukohv similarity theory is valid.

Except for water surfaces, where the temperature is constant throughout the simulation, the surface temperature is calculated by solving the balance equation for the surface heat fluxes with a Newton iteration technique. In the simulations described below, which are characterised as dry, the soil humidity is specified and a prognostic equation is run for the specific humidity, but no condensation occurs.

Together with the boundary conditions, the parameterisation of the turbulence scheme has particular importance for our simulations. For the turbulent diffusion terms the closure assumption from the gradient transport theory is used (Stull, 1988). The values of the eddy viscosity coefficient is computed from a one equation turbulence model, where the eddy viscosity coefficient is parameterised as a function of the turbulent kinetic energy, which is computed by a prognostic equation (Flassak, 1990). The eddy diffusivity for the scalars is then calculated as a relation between the eddy viscosity and the turbulent Prantl number.

The radiative transfer in the atmosphere is computed with an efficient scheme described in Moussiopoulos (1987). The long wave radiation parameterisation scheme is based on the emissivity method, Stephens (1984), and the short wave scheme uses an implicit multi-layer method. The slope of the terrain is included in the computation of the direct solar radiation.

3. Design of the experiments

The motivation for doing the experiments has been given in the introduction and more will be found in the next sections. Here the technical set-up and the physical parameters of the experiments are given. The experiments have all been made with a regular horizontal grid with 5 km grid distance. In all experiments 25 layers have been used vertically with a top at 4000 m. The distance of the layers for the main prognostic variables from the surface has been chosen as follows: 10, 31, 56, 84, 117, 154, 196, 245, 300, 364, 437, 521, 617, 728, 854, 999, 1165, 1355, 1572, 1822, 2108, 2436, 2812, 3243, 3736 m. The distance between the model levels is increasing exponentially with height. The first 10 levels are below 364 m.

Two kinds of experiments have been made:

(1) Experiments, which we have called the narrow channel experiments. This is quasi 2-dimensional experiments in a narrow channel, where the 3-dimensional model has been integrated on a domain with 100×10 points.

(2) The island experiments, which are simulations in summer on a circular island at a latitude at Spitsbergen. The total domain has here covered 60×60 grid points.

The integration domain makes a f-plane, where f is the Coriolis parameter for the latitude in question. All integrations have started with an atmosphere at rest with a constant vertical stability, expressed with the Brunt Väisälä frequency N defined from $N^2 = g/\theta(\mathrm{d}\theta/\mathrm{d}z)$, where θ is the potential temperature. In addition, a constant surface temperature has been given, which is both the SST and the surface ground temperature when the surface is flat. All experiments have been integrated for 36 h.

The channel experiments have been integrated from 18 local sun time (LST), defined at the latitude through the middle of the domain. In the following the time is always LST, but it is indicated by the hour of the day, e.g., 9 h. The date for the experiments has been either 1 April (spring) or 1 July (summer). Surface temperature has been 7°C initially. However, experiments with other surface temperatures have been made. The island experiments have been made for summer only. These integrations started at 6 h in the morning. Surface temperature at sea level has been set to 2°C.

The island experiments have been made on a circular island (or snow/ice cover surrounded by land) with a diameter of 50 km, a scale which should be typical for islands and peninsulas connected to Spitsbergen and Norway. The island has been placed in the middle of the domain. In some experiments an snow/ice cover has been placed in the middle of the island, covering a diameter of 20 km. The model has no scheme to treat melting of snow and ice. In our simulations we have simply not allowed the surface temperature of snow/ice to be higher than 0°C. A grid distance of 5 km might be considered to be too small to resolve the island with the two surfaces. Experiments with higher resolution made by Sandvik (1996) indicate that the resolution is sufficient, except for details of the SB front.

The model has 5 layers below the surface and a constant soil temperature at the bottom. Three kinds of surfaces have been used, we call them sea, land and snow/ice. The characteristics of the experiments, the physical parameters connected to these surfaces and the initial conditions are given in Tables 1 and 2, respectively, for the two types of simulations.

4. Variation of the SB/LB with latitude and season

The variation of the solar insolation at the top of the atmosphere with latitude, season and time

Table 1. *Surface properties and initial conditions in the channel simulations*

Surface properties	0.05 m
land roughness length	0.001 m
ocean roughness length	0.23
land albedo	2.2×10^6 J m^{-3} K^{-1}
soil specific heat capacity	1.3×10^{-6} m^2 s^{-1}
soil thermal diffusivity	
Initial conditions	
land temperature	7.0°C
sea surface temperature	7.0°C
soil temperature at 1.5 m	4.0°C
wind speed	0.0 ms^{-1}
Brunt–Väisälä frequency	0.01 s^{-1}
latitude of the coast	50, 60, 70 or 80°N
starting time	1800 LST
starting day of the year	1 April or 1 July
duration of the simulation	36 h
time step	30 s
Spatial discretisation	
horizontal grid increment	5 km
no. horizontal points	100×10
no. vertical layers	25 (top lev. 4000 m)

Table 2. *Surface properties and initial conditions in the island simulations*

Surface properties	
land roughness length	0.3 m
ocean roughness length	0.001 m
ice roughness length	0.02 m
land albedo	0.23
ice albedo	0.50
soil specific heat capacity	2.2×10^6 J m^{-3} K^{-1}
soil thermal diffusivity	1.3×10^{-6} m^2 s^{-1}
ice specific heat capacity	1.9–10^6 Jm^{-3}K^{-1}
ice thermal diffusivity	1.0–10^{-6} m^{2}s^{-1}
Initial conditions	
land temperature	3.0°C
ice temperature	0.0°C
sea surface temperature	2.0°C
soil temperature at 1.5 m	0.0°C
ice temperature at 1.5 m	−3.0°C
wind speed	0.0 ms^{-1}
Brunt–Väisälä frequency	0.01 s^{-1}
latitude of the centre	78°N
starting time	0600 LST
starting day of the year	1 July
duration of the simulation	36 h
time step	30 s
Spatial discretisation	
horizontal grid increment	5 km
no. horizontal points	60 × 60
no. vertical layers	25 (toplev. 4000 m)

of the day is well known. At equinox day and night have equal length at all latitudes and the daily average insolation varies from zero at the poles and a maximum at the equator. Under spring conditions the SST is relatively high along the coast of Norway and at the western part of Spitsbergen. We will expect a LB, again in concert with terrain-driven circulations, to develop during the night, but normally, a snow cover over land will prevent sufficient heating of the ground for a SB to be developed during the day. Could a SB be developed at high latitudes on a sufficiently large land surface free of snow and ice? Since the insolation during the day is small, the surface temperature might not be sufficiently high, relative to the SST, to develop a SB. In this way we expect a northern limit in spring for the SB to develop.

The change in the insolation from spring to summer is dramatic, and it is a surprise to many how strong the summer insolation is at high latitudes. The daily average insolation at summer solstice is larger at the poles than at equator. Indeed, the largest daily values found on earth are found at the poles (Hartmann, 1994). The strong insolation results from the long days during summer and in spite of the relatively large solar zenith angles. The daily variation of the insolation in summer is small, and at the pole there is no variation at all at summer solstice. The solar conditions naturally result in small daily variations in the heat balance at the surface and surface temperature.

The special solar conditions at high latitudes in summer must have a great effect on the structure of the SB. Let us assume a coast at the north pole with a dry land surface, a relatively cold ocean or an ocean with sea ice, clear sky and no influence of synoptic scale weather. We then expect a steady SB circulation to develop with no diurnal variation. If the land surface had a shape of an island with a sufficient size, a warm monsoon low pressure with constant intensity would follow.

The narrow channel experiments have been made to look further into the nature of high latitude SB/LB circulations indicated above. One purpose has also been to investigate the decrease of the SB/LB extent with the increase in the Coriolis parameter with latitude predicted by theory. As given in Section 3, the experiments have been made for spring and summer and for 50°, 60°, 70° and 80°N respectively. Tests with more grid points in the shortest direction have shown that 10 points are sufficient to avoid errors from the lateral boundaries. Some experiments have been made for typical initial surface temperatures of the season for the different latitudes, keeping the stratification unchanged. They show that initial surface temperature does not play a major rôle in the development of the local circulations. As earlier stated, we have chosen to present the results using the same surface temperature (7°C) for all latitudes and for both spring and summer. Results every third hour have been investigated.

4.1. *Spring*

Characteristic figures of the simulated circulations are found in Table 3, and the variation of the wind at 10 m is shown for the different latitudes in Fig. 2. Like in Arritt (1989), the

Table 3. *Characteristic figures in spring of daily temperature ranges at surface and 10 m (°C), maximum velocity components (ms^{-1}) and extent of the sea breeze (km horizontally, m vertically) at different latitudes of the channel experiments; the maximum values are found at 15 or 18 h (LST); the vertical extent is the depth of the convective boundary layer*

Latitude (°N)	50	60	70	80
range T_s	21	17	13	7
hours when $T_s >$ SST	11	10	6	0
range $T(10\ \mathrm{m})$	11	9	8	4
starting time SB	1100	1300	1500	—
max. wind speed	5.5	3.3	1.3	—
max. wind speed 10 m	4.0	2.8	1.1	—
max. onshore wind speed	4.5	3.0	—	—
max. along-shore wind sp.	1.5	1.0	—	—
tmax. vert. velocity	0.4	0.2	—	—
horizontal extent inland	45	25	10	—
horizontal extent offshore	55	30	10	—
vertical extent	1800	1400	500	—
depth of inflow	750	500	100	—
top of return flow	2500	1500	550	—

extent of the SB over the ocean has been defined from the position where the onshore component of the wind at 10 m is reduced to 1 ms^{-1}. The same limit has also been used for the vertical extent. For the extent of the LB, the limit has been set to 0.5 ms^{-1}.

As expected, there is a large variation of the circulations with latitude. At the lowest latitudes both the SB and the LB are developed, but the strength and extent of the SB decrease rapidly northwards. At 70°N only a weak, small-scaled and shallow SB is present a few hours in the afternoon and the LB is dominating, and at 80°N only the LB is generated. The simulations in this way indicate a northern limit at around 70°N for the SB to develop.

The change of the circulations with latitude can first of all be explained from the diurnal temperature variations at the surface. Fig. 3 shows the temperature variation at the land surface and at 10 m for the four latitudes for a position 20 km from the shore. The temperature change is depending on the starting time at 18 h. The decrease in temperature the first night is naturally the same at all latitudes, and the same minimum temperature is reached at 6 h in the morning. During the day the evolution differs with latitude, and the temperature after 24 h is generally quite different from the starting temperature. In the following, the temperature variation is considered from minimum the first night to minimum the next night.

At the lowest latitudes, there is a small net warming from the first day to the next. The temperature range at the surface is 15°C at 60°N and 19°C at 50°N. The time span for which the land is warmer than the sea surface is 10 h at 60°N and 12 h at 50°N. At 70°N the temperature level does not change much and the diurnal temperature range is 12°C at the surface and 8°C at 10 m. The surface temperature is higher than the SST for 6 h. At 80°N the temperature at the surface is below the SST all the time, indicating a net loss of energy from the surface. There is a small diurnal variation with an estimated temperature range of 7°C at the surface and 4°C at 10 m.

Some details of the structures at the different latitudes will be given. At the lowest latitude, the development is much as in earlier SB/LB descriptions (see references in the introduction). The LB develops during the night and reaches a maximum wind speed of 1.3 ms^{-1}. The effect of the earth's rotation is significant. The largest scale of the LB is found at 6 h in the morning (first day). The LB then reaches 36 km inland and 22 km offshore. Later at 9 h, the LB extends 29 km offshore. The LB then disappears and the SB starts at the coast just before noon. The extent of the SB (50°N) increases steadily during the day. The inward penetration of the SB front is 6.6 km/hour. At 18 h, the SB has reached 50 km inland, and the offshore extent is now 55 km. The maximum wind speed is 3.5 ms^{-1} at 10 m, 10 km behind the SB front. The absolute maximum of 5.5 ms^{-1} is reached two model levels above, at 56 m. At the coast there is also a second weaker maximum at the surface during the day.

The transverse circulation has a marked diurnal variation. It increases in strength and scale until 18 h. The vertical velocity connected to the SB has a maximum of 0.4 ms^{-1} at 15 h. The circulation at 15 h and 18 h is shown in Fig. 4. The convective boundary layer in front of the SB front

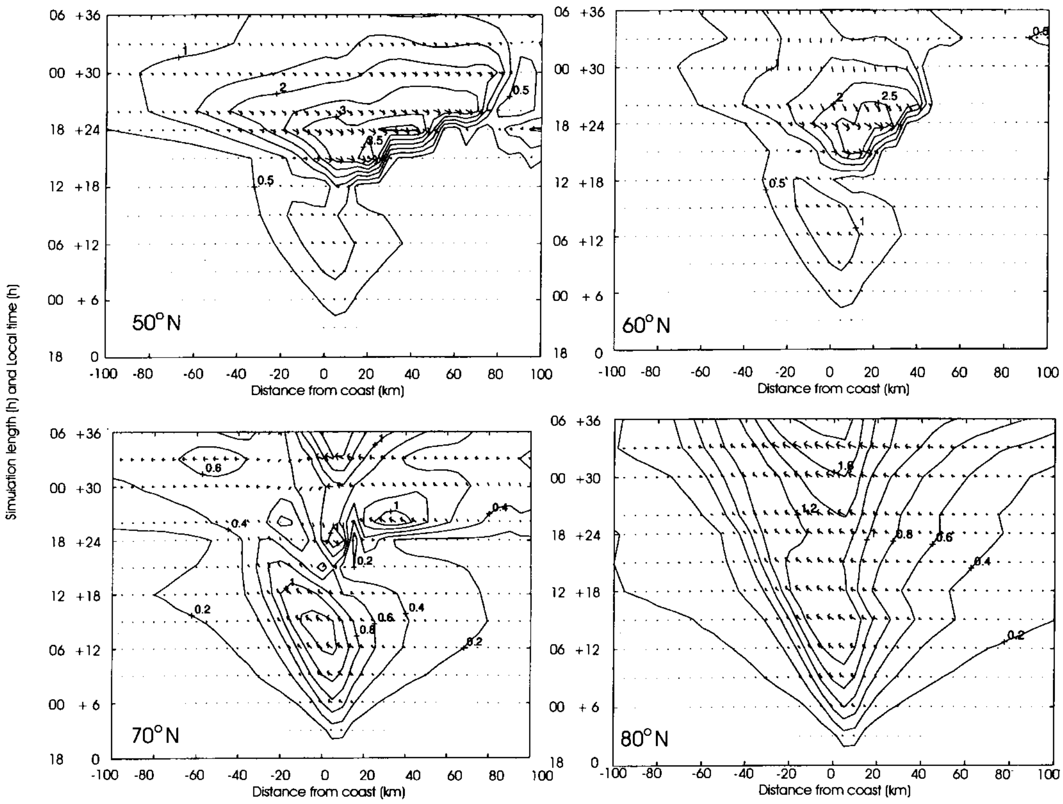

Fig. 2. Daily variation of the wind vector at 10 m in the spring channel simulations at 50°, 60°, 70° and 80°N. Data are given every third hour. Isotacks are also given (ms^{-1}). The vertical axis shows the time of the day and the integration time. The along-shore wind component is along the vertical axis.

reaches 1400 m at 15 h and 1800 m at 18 h. The model seems to be very efficient in establishing the convective boundary layer. Convection cells forms inland and the layer increases until 18 h. The depth of the inward SB reaches 550 m at 15 h and 750 m at 18h. The return current extends up to 2500 m at 18 h, with a maximum speed of 1.5 ms^{-1} between 1200 and 1700 m.

Later in the evening the simulated SB penetrates further inward, but decreases in strength. The along-shore wind component increases from 15 h and is strongest at 21 h. No clear LB is developed the next night. Normally, cumulus clouds are developed over land during the day in situations with SB. These clouds will damp the insolation and contribute to a weakening of the SB. In real cases, we believe that the damping of the SB in the afternoon and night is stronger than in our simulation, giving better conditions for the LB to develop during the night.

At 60°N the SB is considerably weaker. The horizontal extent is nearly halved, and the vertical extent at 18 h is reduced to 1400 m from 1800 m at 50°N. The diurnal variation is much as at 50°N, but since the dying out of the SB is faster, there are signs of a LB the second night. At 70°N the LB is similar to the LB further south, but it lasts longer during the next day. In the afternoon between 15 and 18 h, a very weak SB is noticed. It reaches only 10 km inwards and 10 km offshore. The maximum wind speed is 1.3 ms^{-1}. The next night the LB is a little stronger than the first night (maximum wind speed 1.6 ms^{-1}). At 80°N the LB prevails all the time, becoming a little stronger the second night. The maximum wind speed is constant during the day. The scale of the LB is

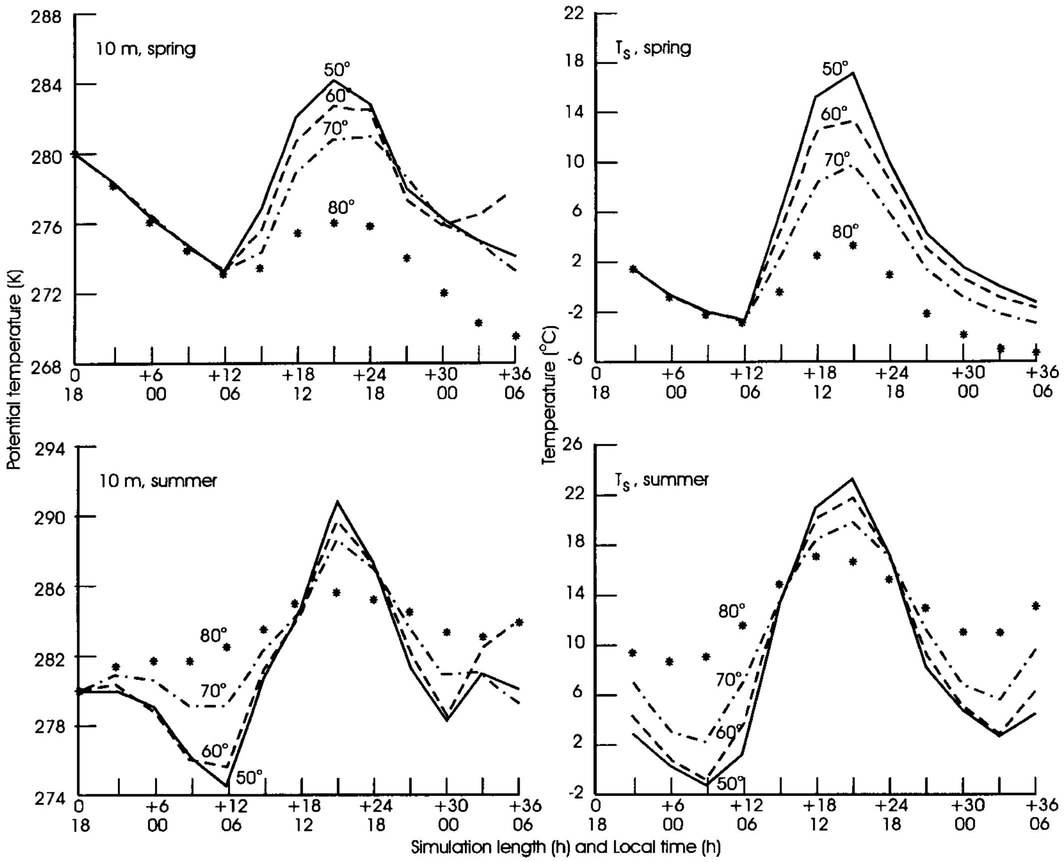

Fig. 3. Daily variation in spring and summer of land surface temperature (°C) and potential temperature at 10 m (K) at a position 20 km from the coast. Curves are given for 50°, 60°, 70°, and 80°N in the channel experiments.

increasing all the time and a monsoon high develops over land. The extent after 36 h simulation is nearly 100 km inland and 100 km offshore.

4.2. *Summer*

Well-developed SBs are now found at all latitudes. Table 4 shows characteristic parameters of the summer simulations and Fig. 5 the variation of the wind at 10 m at 50°N and 80°N. The strength and the extent of the circulation decrease only slightly with latitude. The horizontal extent of the SB inwards from the shore decreases from 95 km (at 18 h) at 50°N, to 70 km at 80°N. Maximum wind speed connected to the circulation is 8.5 ms^{-1} at 50°N, decreasing to 7.0 ms^{-1} at 80°N. The diurnal variation of the SB and LB varies considerably with latitude. At 80°N the SB continue day and night and the LB is absent. The surface pressure is low over land all the time, and in this way a monsoon low is established. At 70°N the SB is dominating, no LB develops, but the first night is characterised with calm conditions with wind speeds less than 0.5 ms^{-1}. Further south the LB is still present at night.

As for spring, the daily variation can be related to the daily variation of the surface temperature. The variation for the four latitudes 20 km inland is shown in Fig. 3 for surface and 10 m. The minimum temperature at the surface the second day is approximately 3°C higher than the first day at all latitudes, indicating a general warming from the first day to the next. The temperature range and the time when the land surface temperature is warmer than the SST change much with latitude. The surface range is 22°C at 50°N, 20° at 60°N,

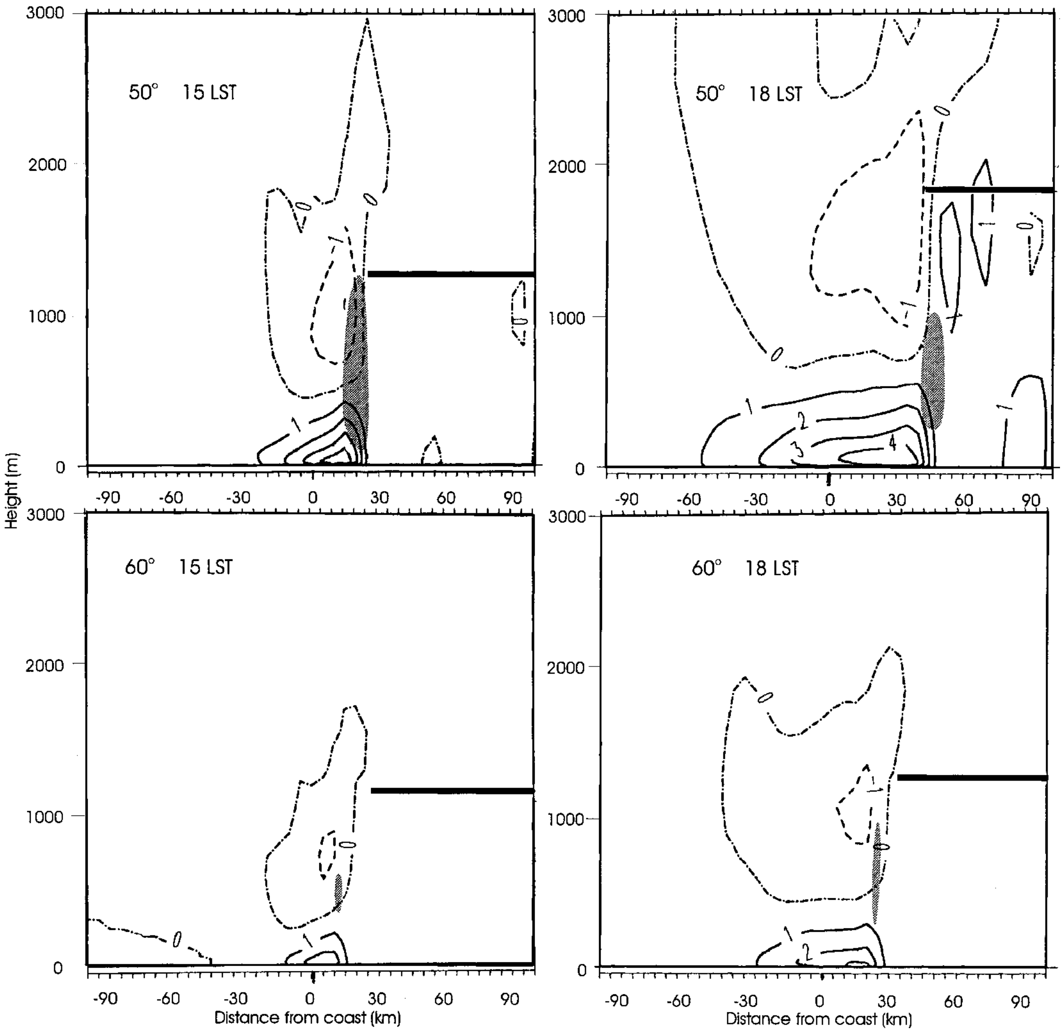

Fig. 4. Cross-section of the transverse circulation (onshore- and vertical wind components, ms^{-1}) at 15 and 18 LST in the channel simulations in spring at 50° and 60°N. Solid lines: positive onshore wind component. The stippled line: negative onshore wind component. Contours every 1 ms^{-1}. Shaded area: vertical velocity equal or greater than 0.2 ms^{-1}. Shown is also the top of the convective boundary layer.

15° at 70°N and 8° at 80°N. At 10 m the ranges are markedly lower, less than 3.5°C at 80°N increasing to 15.5°C at 50°N. The time span with temperature above the SST is 14, 15, 18 and 24 h respectively for the four latitudes.

The SB/LB system at 50° (Fig. 5) and 60°N becomes much stronger than in spring, but the character of the circulation is similar. The horizontal extent of the SB at 50°N is nearly doubled from spring and nearly three times larger at 60°N. The vertical extent has increased to more than 2500 m. A weak LB is still present for some hours during the night.

Since the surface temperature at 80°N is warmer than the SST all the time, a weak SB develops the first evening (Fig. 5). It decreases a little the next morning between 3 and 6 h and redevelops afterwards. The extent increases during the day and has its maximum at 21 h. Then the SB has reached 100 km inwards, and the offshore extent is more

Table 4. *Characteristic figures in summer of daily temperature ranges at surface and 10 m (°C), maximum velocity components (ms^{-1}) and extent of the sea breeze (km horizontally, m vertically) at different latitudes of the channel experiments; the maximum values are found at 15 or 18 h (LST); the vertical extent is the depth of the convective boundary layer*

latitude (°N)	50	60	70	80
range T_s	24	22	18	9
hours when $T_s > \mathrm{SST}$	14	15	18	24
range T(10 m)	16	14	10	4
starting time SB	1000	1000	0900	—
max. wind speed	8.5	8.2	7.0	7.0
max. wind speed 10 m	4.5	4.5	4.2	4.2
max. onshore wind speed	7.2	7.2	6.0	5.2
max. along-shore wind sp.	4.2	4.2	3.5	4.9
max. vert. velocity	1.5	1.0	1.5	1.1
horizontal extent inland	95	85	75	70
horizontal extent offshore	190	125	105	95
vertical extent	2800	2400	2300	2300
depth of inflow	750	750	750	750
top of return flow	3100	3000	2500	2800

than 120 km. A maximum wind speed of 4.2 ms^{-1} (7.0 ms^{-1} at 56 m) is found between 15 and 18 h in connection with the SB front. There is a secondary maximum at the coast. During the night the breeze decreases significantly. However, it does not terminate, and some signs of the SB is present the next morning.

The SB at 70°N is similar (not shown), but the first night phase only gives very weak winds. The SB starts the next morning at 9 h and develops much as at 80°N. The largest extent is at 21 h, but the decrease afterwards is faster than further north. At 6 h the second morning winds at the coast are weak, 0.5 ms^{-1} or less.

The vertical structures of the SB at 18 h, when the transverse circulation is strongest, are shown for 50° and 80°N in Fig. 6a (onshore wind component) and b (along-shore wind component). The results mentioned earlier concerning the scale and the strength are demonstrated. The flow parallel to the coast is strongest at the coast at 50°N, but at 80°N the main maximum is connected with the SB front with a secondary maximum at the coast. We also notice that the lower branch of the return flow is stronger at the northern position. The Coriolis parameter increases 29 % from 50°N to 80°N, and the mentioned differences are probably connected to this change in rotation.

4.3. Discussion

The simulations have shown reasonable variations in the character of the SB/LB circulations

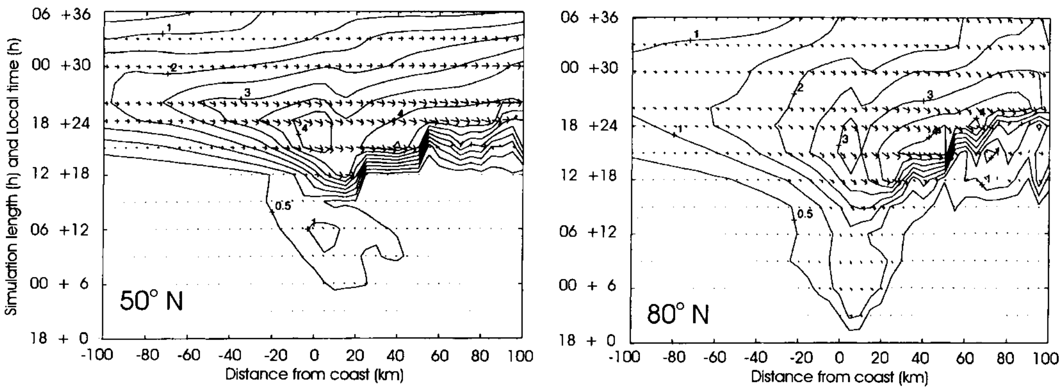

Fig. 5. Daily variation of the wind vector at 10 m in the summer channel simulation for 50° and 80°N. Data are given every third hour. Isotacks are also given (ms^{-1}). The vertical axis shows the time of the day and the integration time. The along-shore wind component is along the vertical axis.

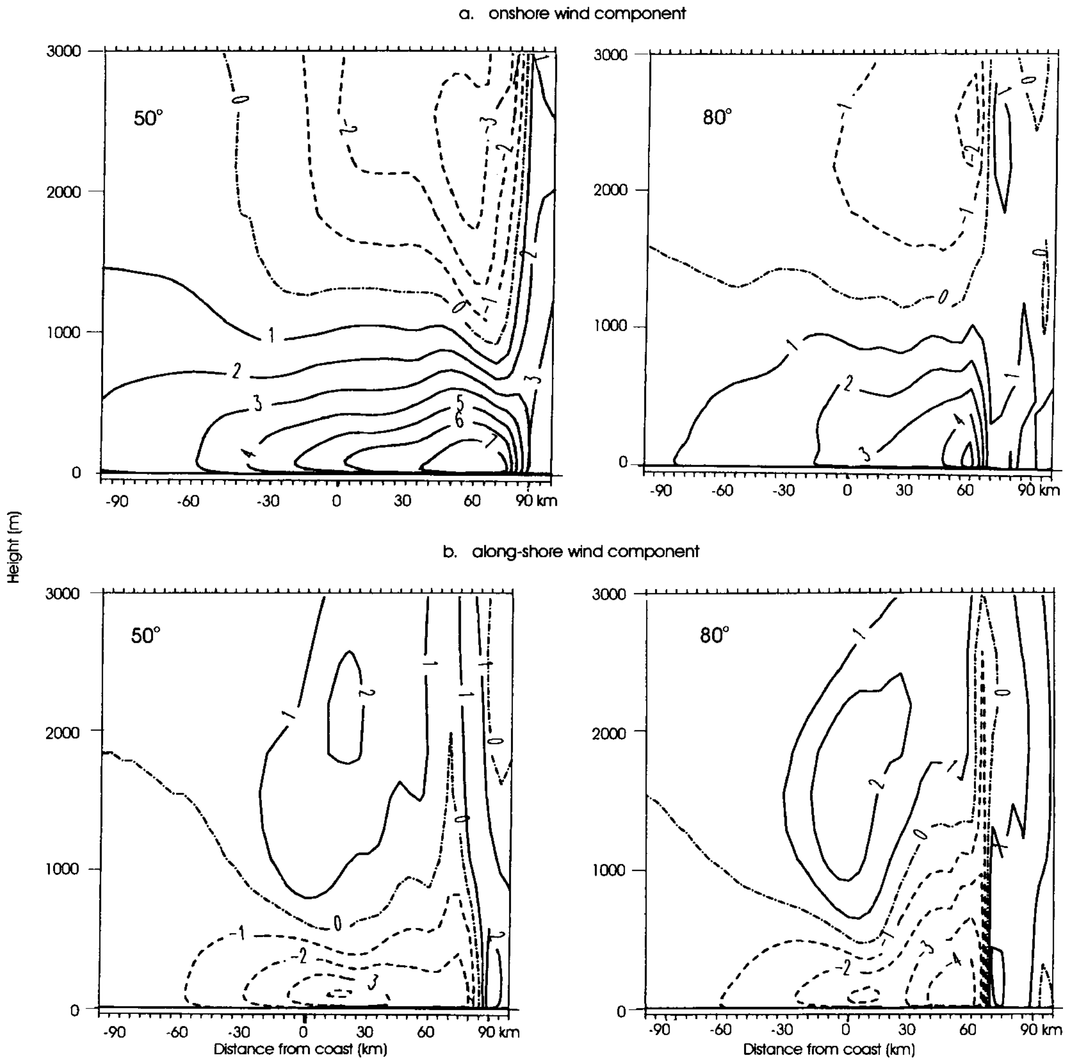

Fig. 6. (a) Cross-section of the onshore wind component (ms^{-1}) at 18 LST in the channel simulations in summer at 50° and 80°N. (b) The along-shore wind component (positive into the paper) at the same latitudes. Solid lines: positive onshore or along-shore wind component. Stippled lines: negative onshore or along-shore wind component. Contours every 1 ms^{-1}.

with latitude and from spring to summer. In spring the extent of the SB decreases markedly with latitude and is absent for the very high latitudes. The LB is present at all latitudes and is dominating at the highest latitudes. In summer the SB is well established at all latitudes and the extent only decreases slightly with latitude. At very high levels it does not terminate during night, and the SB then takes the character of a monsoon low over land. At 60° and 50°N weak LBs are developed. Below we show how these findings compare with observational studies and what role the increase in the Coriolis parameter play for the extent of the circulations.

4.3.1. Comparison with observations. It is generally difficult to compare the results of idealised simulations with observations. In particular, one should also bear in mind — what has been stressed before — that the observed SB often is a combined result of several circulations. The observational evidence has been taken from Grønås and Sandvik (1996). It is known that SBs in spring might develop at 60°N. Further north, no SB has been reported. It is naturally not present at Spitsbergen and not in Tromsø (a town in Norway at nearly 70°N) in early spring (communication with forecasters in Tromsø). However, land surfaces are normally snow-covered in spring at such latitudes and this prevents the heating of the ground. This makes it difficult to estimate from observations any northern limit for LBs to occur under snow-free conditions.

The monsoon SB circulation in summer with on-shore wind at the surface both day and night has been observed in Isfjorden at Spitsbergen in July. Periods lasting for more than 2 weeks have been reported. At 70°N calm conditions were simulated during the night in summer. Also this seems to be in accordance with observational studies in the fjords near Tromsø. Further south, weak LBs are present both in the simulations and the observations.

The speed of the simulated surface wind of the SB seems to be weaker than observed. There might be several good reasons for this. Our simulations include the first day of SB. The monsoon effect seem to give stronger wind the following days. It is known (for references, see Section 5) that the SB becomes stronger in combination with terrain-driven circulations and where the coast forms corners with a sufficient scale (peninsulas). At the coast of Sørlandet (South Norway), the wind becomes stronger because of a frequent large-scale south-westerly flow in the same direction as the SB in the afternoon.

4.3.2. Variation with the Coriolis parameter. It is generally recognised that the following factors affect the structure and extent of the SB/LB circulations: (1) Diurnal variation of the ground temperature, (2) turbulent diffusion of heat (and sometimes momentum), (3) static stability and (4) the Coriolis force.

Rotunno (1983) considered an invisced model of the SB/LB circulations, in which the thermal forcing is present above the land. For latitudes where the Coriolis frequency is larger than the frequency of the day (north of 30°N), Rotunno found that the horizontal extent $L$of the SB varies like:

$$L = Nh(f^2 - \omega^2)^{-1/2} \tag{4.1}$$

Here, f is the Coriolis parameter, ω the frequency of the temperature variation at the ground ($\omega = 2\Pi/(24 \times 3600)$), N the Brunt–Väisälä frequency and h the vertical extent of the SB. Arritt (1987) investigated the variation of the extent of the SB/LB with latitude to 50°N using numerical simulations. He used data from spring and found reasonable agreement with the theory of Rotunno, except around 30°N where the theory breaks down. He also found a variation of the extent with the Brunt–Väisälä frequency in agreement with the theory.

Niino (1987) solved the linear system with turbulent diffusion included. Following his theory, the horizontal dimension of the extent of the combined SB/LB is given by:

$$L = N\kappa^{1/2}\omega^{-3/2}F(f/\omega), \tag{4.2}$$

where κ is the eddy thermal diffusivity and F an universal function of f/ω. F remains constant at a value of 2.2 for latitudes below 30°N. When f becomes larger, F starts to decrease rapidly and becomes equal to 0.9 for $f/\omega = 2$ (the value at the North Pole). The vertical scale of the thermal forcing, h in eq. (4.1), may be regarded as the diffusion length $(\kappa/\omega)^{1/2}$ in eq. (4.2) (Niino, 1987). When this height is kept constant, which indicates no latitudinal variation in the insolation conditions, eqs. (4.1) and (4.2) give estimates of the variation with the Coriolis parameter only. If the extent at 50°N is set to one, the decrease in the extent with latitude according to Rotunno and Niino is shown in Table 5.

The formulae above do not account for latitudinal variation in the insolation. Further, the theories make use of a harmonic component during day and night of the time variation around a mean value (Rotunno specifies the thermal forcing and Niino the surface temperature). This means that neither the experiments in spring, when the insolation varies substantially with latitudes, nor the experiments in summer, when the day is longer than the night, can be directly compared with the theories.

In spring, the simulated decrease of the SB extent with latitude is of course much larger than predicted by the formulas. When the simulated

Table 5. *Latitudinal variation of the horizontal extent of the sea breeze (SB) and land breeze (LB) in percent of the extent at 50°N; theoretical numbers from Rotunno (1983) and (1987) are given for a constant vertical extent and for corrections according to simulated vertical extent in spring; the simulated figures are taken from Tables 3, 4*

Latitude	60°	70°	80°
Rotunno, const. height	85	73	68
corrected for height	66	20	—
Niino, const. height	60	56	53
corrected for height	46	16	—
simulated SB, spring	55	22	—
simulated LB, spring	88	85	87
simulated SB, summer	90	79	73

reduction in the vertical extent of the circulations in spring is introduced in the equations, there is a reasonable agreement between the simulations and the theory (Table 5). The latitudinal reduction of the horizontal extent in the simulations is then found to be between the results in the two theories. The extent of the simulated LB in spring shows a much smaller decrease with latitude. North of 60°N there is nearly any variation at all.

In summer, the mean insolation does not vary much with latitude, but, as mentioned, the harmonic forcing conditions used in the theories do not apply. The horizontal extent in our simulations decreases slightly, but significantly with latitude. We notice that the variation is not far from that in Rotunno's theory.

5. SB circulation on an island at a very high latitude

We have seen how the character of the SB in summer changes from a classical SB at 50°N to a monsoon low SB at very high latitudes with small diurnal variation. We will now make further studies of the high latitude SB from the island experiments at 78°N, which should give a stronger circulation (Neuman and Mahrer, 1974) and a more realistic configuration for Spitsbergen. We first discuss the circulation on a flat island (50 km diameter) free of snow/ice in Subsection 5.1. On islands like Spitsbergen the SB is modified by thermal circulations driven by heating contrasts between snow/ice and dry land and terrain. We investigate the modifying effect on the SB of an ice-cover and a mountain from two experiments: a flat island experiment with an ice-cover in the middle and the same experiment with mountains included. The results are given in Subsection 5.2. As we remember, the integrations started at 6 h in the morning and are run for 36 h. The characteristics of the three experiments are given in Table 5.

5.1. SB circulation on a flat island

The small diurnal variation of the heating over the island gives a monsoon low SB circulation with low pressure over the island both day and night.

5.1.1. The flow at the surface. The wind and temperature evolution at the surface is found for a cross-section through the centre of the island in Fig. 7. The wind at 56 m (Fig. 7c) represents maximum wind speed in the circulation, which is found from this level and a few hundred meters upwards. The temperature is raised 5°C over the middle of the island and the maximum temperature is found at 15 h. A SB is developed which penetrates steadily inwards and reaches the centre of the island at 15 h. With the development of the inward wind, the Coriolis force acts to produce a component to the right. The influence increases during the first hours and the wind direction is veering as expected. A maximum wind speed of 7.0 ms^{-1} is found between 15 and 18 h at a position 10 km from the centre. A secondary maximum develops off the coast with the same strength as the first maximum at 10 m (Fig. 7b). This shallow maximum can partly be explained by less friction above the sea surface.

After 15 h, the wind direction is steady until midnight and the maximum wind decreases 2 ms^{-1} to 5 ms^{-1}. Off the coast, the wind direction at the surface makes an angle of 20° with the coastline. Inland, this angle increases to more than 45° at the surface. During the night, the drop in the temperature is small, only 3°C or less over the island. As for the channel experiments, the temperature is all the time significantly higher than the SST, and the next morning there is still a negative pressure anomaly over land. Maximum wind speed over land at 56 m decreases steadily to 3 ms^{-1} at 6 h the next morning. The wind max-

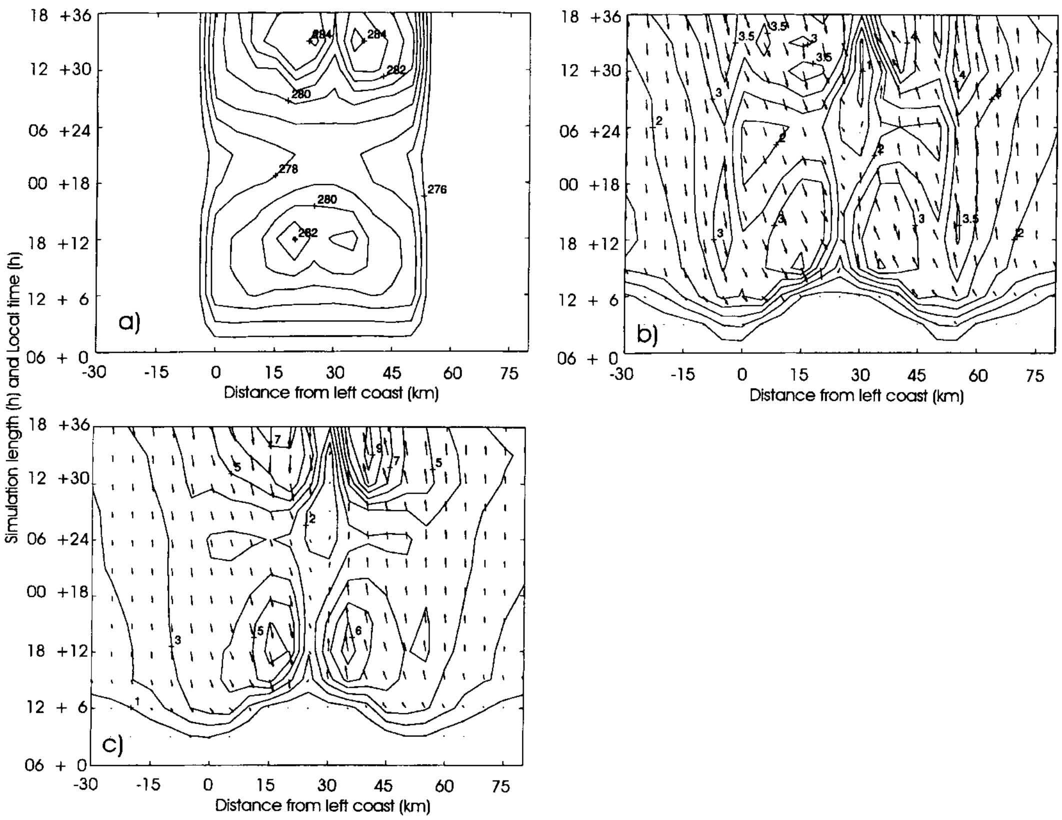

Fig. 7. Daily variation of temperature and wind near the surface in the island experiment in summer with no ice, along an axis across the island: (a) potential temperature (K) at 10 m, (b) wind vector at 10 m and c) wind vector at 56 m. The data are given every third hour. Isotacks are also given (ms^{-1}). The vertical axis shows the time of the day and the integration time. The along-shore wind component is along the vertical axis.

imum off the coast is present all the time with nearly no change in the wind direction. The wind speed is only reduced from 3.5 ms^{-1} the first day to 3.0 ms^{-1} the next morning.

The next day starts with higher temperatures than the first day and the maximum temperature becomes 2°C higher. The circulation becomes stronger with a maximum speed of 9 ms^{-1} at 56 m. The symmetry of the flow is now less distinct than the first day and has a more spiralling structure. The wind speed at the coastal maximum increases on the second day to 4.3 ms^{-1} at the surface. There seems to be an inward penetration of the SB also the second day, superimposed on the heated island circulation present in the morning. We notice that the offshore extent of the circulation is large, twice the radius of the island.

5.1.2. The 3-dimensional flow. In a circular vortex the transverse circulation represents the divergent wind and the azimuthal wind component the rotational wind. The transverse circulation at 15 h the first day and the next is shown in a cross-section in Fig. 8, and the wind component along the coast is shown in the same cross-section in Fig. 9 for 18 h at the two days and at 6 h the second morning. The start of the SB is classical. The heat source gives a high aloft and an outward directed pressure gradient. The outward directed force produces divergence which removes mass from the centre, resulting in surface pressure falls. The associated low produces convergence, which together with the divergence aloft produces the transverse circulation. The divergence aloft is slightly stronger than the convergence below and

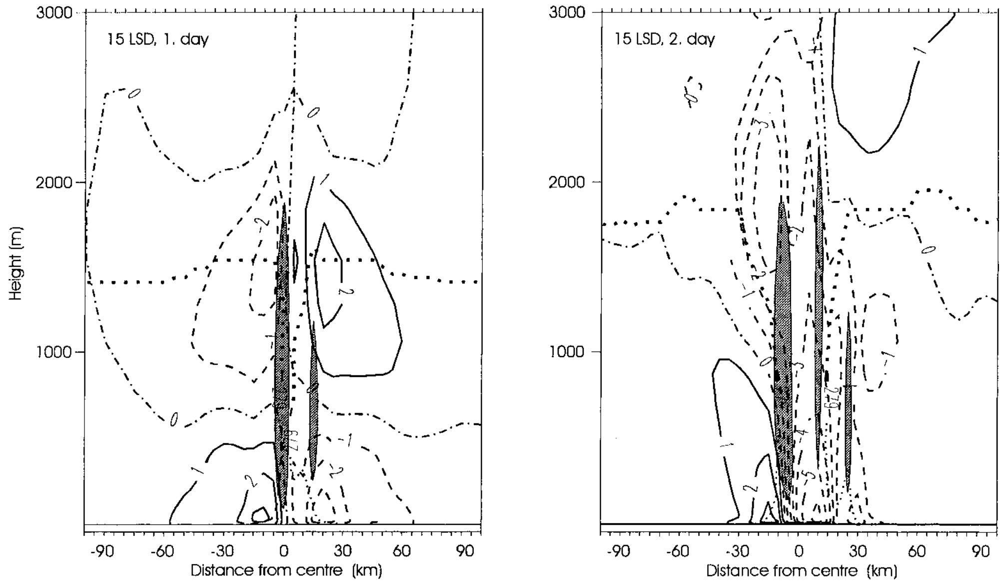

Fig. 8. Cross-section of the transverse circulation (onshore- and vertical wind component (ms^{-1})) at 15 LST in the island experiment with no ice. Left: the first day, right: the second day. Solid lines: positive onshore wind component. Stippled lines: negative onshore wind component. Contours every 1 ms^{-1}. Shaded areas: vertical velocity greater than 0.2 ms^{-1}. One isotherm of the potential temperature (279 K) is also shown as a dotted line.

the surface pressure is falling. During this process, the Coriolis effect acts on the divergent transverse wind to produce a rotational wind which is anti-cyclonic aloft and cyclonic below. When the SB has penetrated to the middle of the island, the circulation takes form of a heated island circulation. The cyclonic vortex at the surface is increased in depths at the centre, and the anti-cyclonic vortex aloft is found in a ring outside this circulation.

The transverse circulation has a distinct diurnal variation, which follows the daily variation in the heating of the island. The first day the circulation is strongest between 12 and 15 h with maximum inflow at the surface (to about 500 m at 15 h and maximum 3.5 ms^{-1}, Fig. 8, left) and with maximum vertical velocity at the centre (1.0 ms^{-1}). The outflow in the layer above reaches 1900 m, with the strongest outflow between 900 to 1500 m. The transverse circulation decreases rapidly after 18 h and is weak downward or absent between 21 h and 6 h the next morning. The next day the circulation grows higher and stronger (Fig. 8, right). As mentioned, there is also now a SB front circulation moving inwards, superimposed on the heat island circulation. After midday there are several cells of vertical velocity, reflecting a less organised flow.

The heating of the surface develops a boundary layer with neutral static stability. The first day the neutral layer reaches a maximum height of 1700 m at 15 h (Fig. 8, right). Potential temperature in this layer is close to 279 K, except for a warmer layer close to the surface indicating static instability. Except for some stabilisation in this surface layer, the neutral layer persists during the night. The next day the warming is more extensive and the neutral layer is raised to 2700 m (Fig. 8, right), at a potential temperature of 279.5 K.

The cyclonic vortex is formed by the influence of the Coriolis force on the inflow as the transverse circulation is developed. The vortex extends through the neutral layer. The strongest winds the first day are found in the lowest 350 m. The vortex is strongest at 18 h when the maximum azimuthal wind component is 6.5 ms^{-1} (Fig. 9, upper left and lower left). The cyclonic vortex decreases steadily during night due to a maximum speed of 3.0 ms^{-1} the next morning (Fig. 9, upper right). Since the cooling during night is small and the

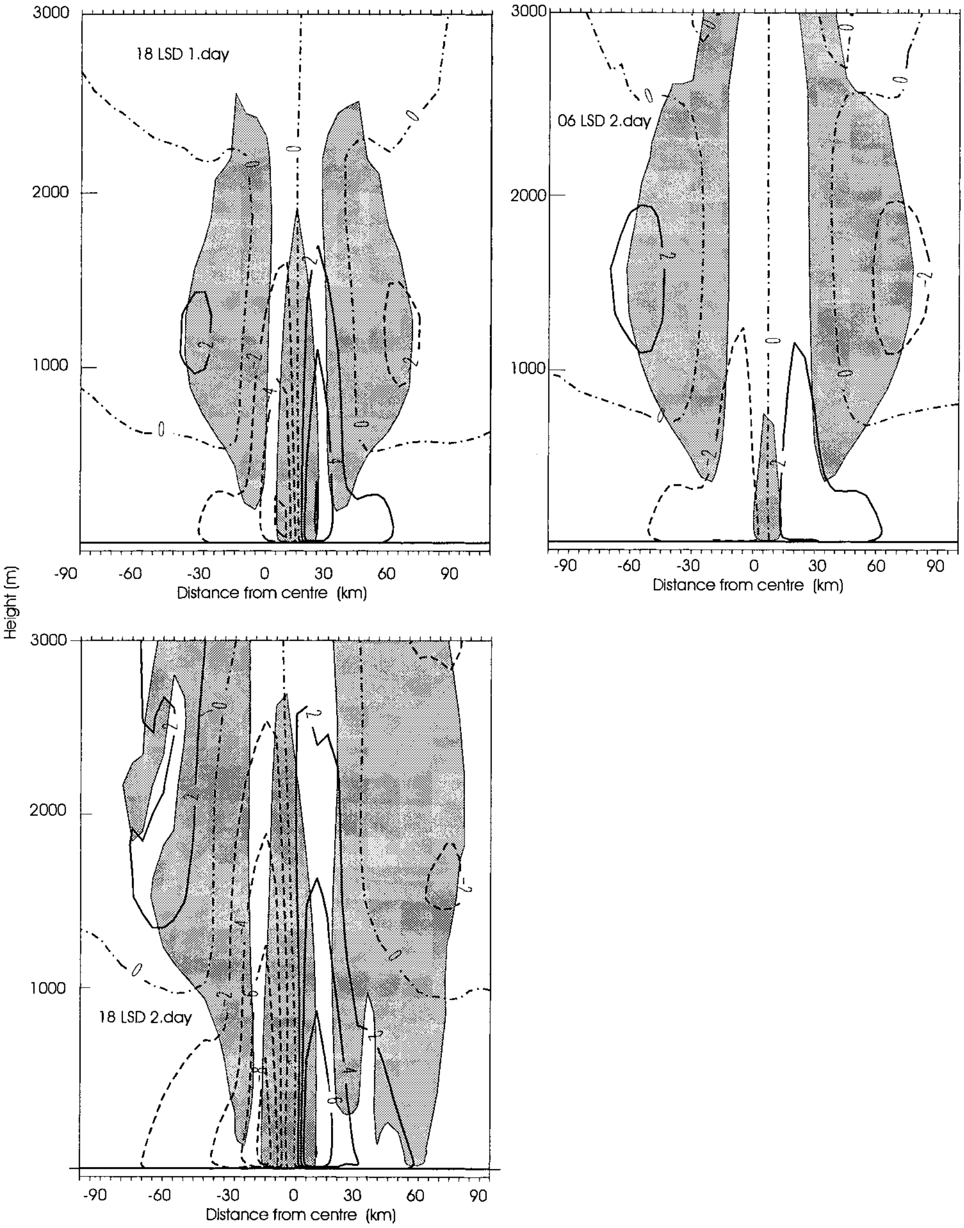

Fig. 9. Cross-section of the along-shore wind component in the circular island experiment with no ice at 18 LST the first day (upper left), 06 LST the second day (upper right) and 18 LST the second day (lower left). Lines: the along-shore wind component, contours every 2 ms^{-1}, solid: positive values (into the paper), stippled lines: negative values. Hatched areas: negative vorticity and positive vorticity greater than 0.0005 s^{-1}.

transverse circulation more or less is absent, the decrease of the strength of the vortex seems to be caused primarily by surface friction. The anti-cyclonic vortex aloft extends through a deep layer and the negative vorticity is found as a ring outside and over the cyclonic vortex (Fig. 9, upper panel). The vorticity change of the anti-cyclonic vortex is small during the night. The maximum azimuthal component is found between 1000 and 2000 m with a maximum speed of 2.5 ms^{-1}. The next day the cyclonic vortex intensifies and penetrates a deeper layer (Fig. 9, lower panel). Also the anticyclonic vortex extends further upward.

5.2. *Modification of the SB circulation by an snow/ice-cover*

We refer to Table 6 for characteristic figures of the SB for this island simulation. The SB circulation is much as in the experiment without the snow/ice-cover. The main effect of the snow/ice cover on the SB is a delay in the inward penetration of the SB. The extent and strength of the SB circulation is also slightly smaller.

A SB starts to develop near the coast and the snow/ice breeze at the snow/ice edge. Over the land area free from snow/ice the warming is much as in the case with no snow/ice cover. The temperature in the middle is nearly constant, but decreases 3°C during the night. As in the no snow/ice experiment, the temperature becomes 2°C warmer the second day. At noon the inward SB and the outward snow/ice breeze meet. Later, the combined breeze continues to penetrate slowly inwards (1.3 km/h) and passes the snow/ice edge. The inward penetration continues until midnight, but does not reach the middle. Over the snow/ice the wind at the surface is more parallel with the coast than in the case with no snow/ice. This is partly due to less surface friction over the snow/ice.

The wind speeds are slightly weaker than with no snow/ice cover in the middle and the horizontal extent slightly smaller. The coastal maximum is very much as in the first experiment.

Table 6. *Characteristic figures of temperature (°C), maximum velocity components (ms^{-1}) and extent of the sea breeze (km horizontally and m vertically) in summer at 78°N*

Simulation		1	2	3
maximum T(10 m)	day 1	9.2	6.9	7.2
	day 2	11.2	9.5	10.5
maximum wind speed	day 1	6.7	4.8	5.2
	day 2	8.8	8.4	8.6
maximum wind speed 10 m	day 1	3.6	3.2	3.8
	day 2	4.2	4.8	5.4
maximum wind speed at the coast at 10 m	day 1	3.2	3.2	3.2
	day 2	4.0	4.0	4.0
maximum onshore wind component	day 1	3.4	3.1	3.4
	day 2	4.3	3.4	3.6
maximum along-shore wind component	day 1	6.3	4.3	4.9
	day 2	7.7	7.9	8.1
maximum vertical velocity	day 1	1.0	0.7	0.6
	day 2	1.0	1.0	0.7
horizontal offshore extent	day 1	55	50	50
	day 2	75	70	70
vertical extent	day 1	1800	1400	1500
	day 2	3100	3000	3000

The maximum values are taken at 15 or 18 h (LST). The experiments have been made on a circular island with a diameter of 50 km. Simulation 1: flat island, no snow. Simulation 2: flat island, snow in the middle. Simulation 3: mountainous island, snow at the top. The vertical extent is the depth of the convective boundary layer.

5.3. *Modifications of the SB circulation by a mountainous and an snow/ice-covered top*

This experiment is closest to real conditions at high latitudes like Spitsbergen. The generated circulation is very similar to the circulation in the experiments with a flat island with and without snow/ice described earlier. In particular, the flow off the coast with the coastal maximum is similar in strength and extent. Compared with the flat island experiment with snow/ice in the middle, the circulation is a little stronger. This is in agreement with what is found by others on the effect of topography (Mahrer and Pielke, 1977).

There are some differences compared to the no snow/ice, no mountain experiment. The penetration of the breeze inwards is slower than in the first experiment, but not as slow as in the flat island case with snow/ice in the middle. As before the wind over the snow/ice is weak and more normal to the coast (less friction). It is interesting that of all the experiments, this experiment gives the best symmetry of the flow the second day. The symmetry is there in spite of the variation of the surface temperature on the slopes with changing azimuth angle (not shown).

5.4. *Discussion*

Our island gives wind speeds at the surface only marginally stronger than at the straight coast. Neuman and Mahrer (1974) has shown that island circulations are generally significantly stronger due to the additional convergence provided by the island flow. However, the strength of the circulation is depending on the size of the island. According to theoretical studies by Niino (1987) and numerical simulations by Mahrer and Segal (1985), there is a minimum size of an island for SB circulations to be formed and the strength of the circulation increases with the size of the island for islands up to a maximum size. Our island (50 km width) is large enough for the SB to develop, but too small to obtain a maximum strength. The SB penetrates quickly to the centre of the island and the radius is far less than the extent of the SB at straight coast (70 km at 80°N). The efficiency of the island circulation might in our case be illustrated by the offshore extent, which is more than twice the radius of the island.

The island simulations with a 20 km wide snow/ice cover in the middle and the introduction of mountains do not make essential changes of the SB circulations. Especially, the flow at the coast and off the coast is nearly not changed at all. The small extent of the snow/ice cover prevents the SB front from reaching the centre of the island and the mountains increase the maximum wind speed a little. Further studies of terrain-driven circulations combined with circulation driven by changes in the surface type is needed. At high latitudes, circulations between snow/ice ground and dry land surfaces should be given more attention. Some results might be found in Grønås and Sandvik (1996). Although the diurnal variation in the insolation is small, it should be remembered that the azimuth angle of the sun has a diurnal variation with a large zenith angle. For small scaled mountains, this must give large diurnal variation of the smaller scale circulations connected to the slopes. The fact that some slopes might be covered with snow/ice and some are dry might give complicated circulations.

Traditionally, simulations of SB/LBs have been made for 24 h from initial conditions in a state of rest at a time with little insolation and little wind. In our summer cases a significant insolation has been present at the highest latitudes at the start of the integrations. Ideally, there should also have been a circulation initially in balance with the heating. Alternatively, the integration could be made for additional days to obtain a steady solution from one day to the next. Our integrations for 36 h are probably too short to obtain such a balance. However, we think our simulations demonstrate the main character of the development. Real case integrations are indeed desirable to study the building up of SB monsoon lows.

6. Summary and concluding remarks

Studies of high latitude sea and land breeze (SB/LB) are very few. However, as shown in a summary of investigations at some Norwegian institutions recently made by Grønås and Sandvik (1996), such circulations are common in Norway and have also been observed at Spitsbergen at nearly 80°N. The SB/LB circulations along the coast of Norway in spring and summer, and at Spitsbergen in summer, are complex phenomena driven by surface heat contrasts and terrain. At times and particularly in spring, the SB/LBs also work together with similar circulations formed at surface contrasts between land and snow surfaces. The character of the SB/LB circulations seems to vary considerably with latitude and change dramatically from spring to summer along with the large increase in the insolation. Over South Norway classical SB/LB systems are frequent in summer. In spring, the systems have smaller scales, and they work normally in concert with circulations formed between snow-covered mountains and dry ground at the coast. Further north the SBs seem to be present only in summer, and at Spitsbergen SBs have only been observed in July. There is obviously a need to get a better understanding of the phenomena indicated in few reports summarised by Grønås and Sandvik (1996). In this paper the variation of high latitude SB/LB circulations with latitude and season has been studied from numerical simulations with a non-hydrostatic model with a horizontal grid distance of 5 km and with 25 layers below the top at 4 km.

Simulations have been made on a straight coast for spring and summer, the only seasons when SB might be generated at high latitudes. The simulations show that in spring, when the insolation decreases rapidly with latitude, there is also a marked decrease with latitude in the extent and strength of the SB/LB circulations. The inland extent and maximum wind speed at the surface are nearly halved from 50° to 60°N. At 70°N there is just a weak indication of the SB in the afternoon, and further north no SB is present at all. The LB is found at all latitudes, at 70°N it is dominating and at 80°N it is present both day and night and grows in strength from the first day to the next. Observational studies indicate that SBs are developed in early spring at 60°N. Further north no SBs have been reported, probably because the ground normally is covered with snow which prevent the solar heating. It is found that the simulated horizontal extent of the SB decreases with increasing Coriolis parameter, and the estimated decrease is found to be between the results predicted by theories of Rotunno (1983) and Niino (1987).

In summer, when the average diurnal insolation is surprisingly high, the simulated SBs are well developed at all latitudes. The character of the SB changes from a classical SB at the lowest latitudes to a what we have called a monsoon low SB at the very highest latitudes, characterised by low pressure over land both day and night and small diurnal variation in the wind at the coast. Accordingly, the monsoon low SB does not terminate during the night. There is just a small decrease in summer in the horizontal extent and strength of the SB with latitude, caused by the increased rotation. The LB is present at 50° and 60°N. At 70°N the nocturnal winds are very weak. The monsoon low SB further north at 80°N is in agreement with observations at Spitsbergen in July.

The monsoon low SB circulation in summer at very high latitudes has been further studied from simulations on a circular island (50 km width, at 78°N), a configuration which is more realistic for Spitsbergen. The circular shape of the coast gives low-level convergence to the flow (Neuman and Mahrer, 1974) and strengthens the circulation compared to that on a straight coast. In our simulations the strong circulation is for instance indicated by the offshore extent of the flow, which is more than twice the radius of the island. The simulations show a marked circulation above the heated island which persists during the night and grows in extent and strength from the first day to the next. The flow is characterised by a cyclonic vortex near the surface and an anti-cyclonic return vortex above and outside the heated air. The transverse circulation has a distinct diurnal variation. During the day, there is a marked inflow at the surface and outflow aloft, and this circulation ceases in the evening. The surface wind at the coast has a substantial component parallel with the coast and shows only a weak diurnal variation in accordance with observations at Spitsbergen. Modifying effects of an snow/ice cover in the middle of the island (20 km width) and mountains (600 m high) do not change the essence of the SB circulation. Especially, the conditions at the coast and off the coast are very similar. However, the snow/ice cover prevents the inward penetration of the SB and relatively large vertical velocities are found between the SB and the circulation forced by the snow/ice land heating contrasts. In this respect the flow is similar to situations indicated already by Bergeron (1934) and illustrated in a case by Grønås and Sandvik (1996) from South Norway during a day in spring. In the simulations the dimension of the snow/ice cover is small compared to the extent of the SB. The relative importance of the snow/ice cover will generally vary much with its extent.

Observations from Spitsbergen (Grønås and Sandvik, 1996) indicate that a monsoon low might be present for many days in July. Synoptic experience (Godske et al., 1957) seem to indicate that such lows also might be formed over islands and peninsulas at lower latitudes like Iceland and South Norway. Such indications were not found in the straight coast simulations. However, the strong nocturnal cyclonic circulation at the surface found on the island at 78°N, suggests that such monsoon lows also might be established further south. Indeed, numerical simulations by two students of Grønås (S. Dearsley and A. Tjøstheim, master theses in Norwegian, 1993), with a hydrostatic model on peninsulas and coasts, show very weak cyclonic flows just off the coast during the night at least down to 60°N.

The simulated SB/LBs were generated from a state of rest at a particular time of the day and the integrations went also into a second day. In this way the initial conditions have not been in balance with the heating (cooling) of the surface. A change was observed in the circulations from the first day to the next, for instance, the monsoon low SB increased in strength the second day. Because of the initial imbalance, we can not be sure how much of this change which is real. The building up of monsoon low SBs should be studied in longer integrations to obtain stable circulations from one day to the next. Such integrations should also include wet processes, since latent heat release might modify the character of the SB. Further observational studies on monsoon lows SB are also needed. Such studies should go along with real case numerical predictions.

The circulations connected to heat contrasts between snow/ice and dry land should also be further investigated. A few results might be found in Grønås and Sandvik (1996). Although diurnal variation in insolation in summer is small, the turning of the azimuth angle during the day at high zenith angles makes large diurnal variations in the insolation on slopes. It is anticipated that complicated smaller scale circulations might occur, in particular, when some slopes are covered with snow/ice and some are dry.

7. Acknowledgements

Discussions with Dr. T. E. Nordeng, Professor H. Sundqvist, and Associate Professor Elmer Raustein are appreciated. We also wish to thank Mr. F. Cleveland for his assistance in drawing the figures. The super-computing time has been made available by The Norwegian Research Council.

REFERENCES

Anthes, R. A. 1978. The height of the planetary boundary layer and the production of circulation in a sea breeze model. *J. Atmos. Sci.* **35**, 1231–1239.

Arritt, R. W. 1989. Numerical modelling of the offshore extent of sea breezes. *Quart. J. Roy. Meteor. Soc.* **115**, 547–570.

Atkinson, B. W. 1981. *Mesoscale atmospheric circulation.* Academic Press, 495 pp.

Bergeron, T. 1934. *Die dreidimensional verknüpfende Wetteranalyse. II. Dynamik und Thermodynamik der Fronten und Frontalstörungen.* Ausg. Zentralverw. Hydro-meteor. Einheitsdienstes (Moscow).

Carpenter, K. M. 1982. Note on the paper 'Radiation condition for the lateral boundaries of limited area numerical models', by M. J. Miller and A. J. Thorpe, 1982, Q.J., 107, 615–628. *Quart. J. Roy. Meteor. Soc.* **108**, 717–719.

Copson, E. T. 1975. *Partial differential equations.* Cambridge University Press, 280 pp.

Deardorff, J. W. 1978. Efficient prediction of ground surface temperature and moisture with inclusion of a layer of vegetation. *J. Geophys. Res.* **83**, 1889–1903.

Estoque, M. A. 1961. A theoretical investigation of the sea breeze. *Quart. J. Roy. Meteor. Soc.* **87**, 136–146.

Estoque, M. A. 1962. The sea breeze as function of prevailing synoptic situation. *J. Atmos. Sci.* **19**, 244–250.

Estoque, M. A. and Gross, J. M. 1981. Further study of a lake breeze. Part II: Theoretical study. *Mon. Wea. Rev.* **109**, 619–634.

Flassak, T. 1990. *Ein nicht-hydrostatisches mesoskaliges modell zur beschreibung der dynamik der planetaren grenzschicht*. Forrtschr.-Ber. VDI Reihe 15, VDI-Verlag, Düsseldorf, 203 pp.

Flassak T. and Moussiopoulos, N. 1987. An application of an efficient non-hydrostatic mesoscale model. *Boundary Layer Met.* **41**, 135–147.

Godske, C. L., Bergeron, T., Bjerknes, J. and Bundgaard, R. C. 1957. *Dynamic meteorology and weather forecasting*, pp. 592–595, 800 pp., A.M.S., Boston, Mass., U.S.A.

Grisogono, B. and Tjernstroem, M. 1996. Thermal mesoscale circulation on the Baltic coast. 2. Perturbation of surface parameters. *J. of Geophys. Res.* **101**, 18999–19012.

Grønås, S. and Sandvik, A. D. 1996. An analysis of sea and land breezes at high latitudes based on numerical simulations. In, *Condensation processes in a non-hydrostatic mesoscale model.* PhD thesis, Geophysical Institute, University of Bergen, Norway.

Hanssen-Bauer, T., Kristensen Solås, M. and Steffensen, E.L. 1990. *The climate of Spitsbergen.* Klima, Report 39/90, The Norwegian Meteorological Institute, Norway.

Harten, A. 1984. On a class of high resolution total-variation-stable finite-difference schemes. *SIAM J. Number. Anal.* **21**, 1–23.

Harten, A. 1986. On a large time-step high resolution scheme. *Math. Comp.* **46**, 379–399.

Hartmann, D. L. 1994. *Global physical climatology*. Academic Press, 410 pp.

Johnson, R. H., Young, G. S., Toth, T. J. and Zehr, R. M. 1984. Mesoscale weather effects of variable snow cover over north-east Colorado. *Mon. Wea. Rev.* **112**, 1141–1152.

Kikuchi, Y., Arakawa, S., Kimura, F., Shirasaki, K. and Nagano, Y. 1981. Numerical study on the influence of mountain on the land and sea breezes circulations in the Kanto district. *J. Meteor. Soc. Japan* **59**, 723–738.

Klemp, J. B. and Durran, D. R. 1983. An upper boundary condition permitting internal gravity wave radiation in numerical mesoscale models. *Mon. Wea. Rev.* **111**, 430–444.

Kunz, R. and Moussiopoulos, N. 1995. Simulation of the wind field in Athens using refined boundary conditions. *Atmos. Env.* **29**, 3575–3591.

Mahrer, Y. and Pielke, R. A. 1977. The effect of topography on sea and land breezes in a 2-dimensional numerical model. *Mon. Wea. Rev.* **105**, 1151–1162.

Mahrer, Y. and Segal, M. 1985. Notes and correspondence on the effects of islands geometry and size on including sea breeze circulations. *Mon. Wea. Rev.* **113**, 170–184.

McPherson, R. D. 1970. A numerical study of the effect of a coastal irregularity on the sea breeze. *J. Appl. Meteor.* **9**, 767–777.

Moussiopoulos, N. 1987. An efficient scheme to calculate radiative transfer in mesoscale models. *Environmental Software* **2**, 172–191.

Moussiopoulos, N. 1989. Mathematische modellierung mesoskaliger ausbreitung in der Atmosphere. VDI Verlag, Düsseldorf, Germany, 307 pp.

Moussiopoulos, N. 1994. The EUMAC zooming model, model structure and application. EUROTRAC International Scientific Secretariat, Garmich-Partenkirchen, Germany, 266 pp.

Neuman, J. and Mahrer, Y. 1971. A theoretical study of the lake and land breezes of circular lakes. *Mon. Wea. Rev.* **103**, 474–485.

Neumann, J. and Mahrer, Y. 1974. A theoretical study of the sea and land breezes on circular islands. *J. Atmos. Sci.* **31**, 2027–2039.

Neumann, J. and Mahrer, Y. 1975. A theoretical study of the lake and land breezes of circular lakes. *Mon. Wea. Rev.* **103**, 474–485.

Neuman, J. and Savijärvi, H. 1986. The sea breeze on a steep coast. *Beitr. Phys. Atmosph.* **59**, 375–389.

Niino, H. 1987. Linear theory of land and sea breeze circulation. *J. Meteor. Soc, Japan* **65**, 901–920.

Oerleman, J. and Vugts, H. F. 1993. A meteorological experiment in the melting zone of the Greenland ice sheet. *Bull. Amer. Soc.* **74**, 355–365.

Ookouchi, Y., Uryu, M. and Sawada, R. 1978. A numerical study on the effect of a mountain on the land and sea breezes. *J. Meteor. Soc. Japan* **56**, 368–385.

Ookouchi, Y. and Wakata, Y. 1984. Numerical simulation for the topographical effect on the sea-land breeze in the Kyushu Island. *J. Meteor. Soc. Japan* **62**, 864–879.

Orlanski, J. 1976. A simple boundary condition for unbounded hyperbolic flows. *J. Comput. Phys.* **21**, 251–269.

Pearce, R. P. 1955. The calulation of sea breeze circulation in terms of the differential heating across the coastline. *Quart. J. Roy. Meteor. Soc.***71**, 351–381.

Physick, W. L. 1976. A numerical model study of sea breeze phenomenon over lake or gulf. *J. Atmos. Sci.* **33**, 2107–2135.

Physick, W. L. 1980. Numerical experiments on the inland penetration of the sea breeze. *Quart. J. Roy. Meteor. Soc.* **106**, 735–746.

Pielke, R. A. 1974. A 3-dimensional numerical model of the sea breeze over south Florida. *Mon. Wea. Rev.* **102**, 115–139.

Rotunno, R. 1983. On the linear theory of the land and sea breeze. *J. Atmos. Sci.* **40**, 1999–2009.

Sandvik, A. D. 1996. Condensation processes in a non-hydrostatic mesoscale model. PhD. Thesis. Geophysical Institute, University of Bergen, Norway, 182 pp.

Segal, M. and Arritt, R. W. 1992. Nonclassical mesoscale circulations caused by surface sensible heat-flux gradients. *Bull. Amer. Soc.* **73**, 1593–1604.

Simpson, J. E. 1994. *Sea breeze and local winds.* Cambridge University Press, 228 pp.

Stephens, G. L. 1984. The parameterization of radiation for numerical weather prediction in a climate model. *Mon. Wea. Rev.* **112**, 826–867.

Stull, R. B. 1988. *An introduction to boundary layer meteorology.* Kluwer Academic Publisher, 666 pp.

Tjernström, M. and Grisogono, B. 1996. Thermal mesoscale circulation on the Baltic coast. 1. Numerical case study. *J. of Geophys. Res.* **101**, 18979–18997.

Yan, H. and Anthes, R. A. 1986. The effect of latitude on the sea breeze. *Amer. Met. Soc.* **115**, 936–956.